Published in final edited form as:
Microcirculation. 2011 July ; 18(5): 380–389. doi:10.1111/j.1549-8719.2011.00099.x.

Bifurcations: Focal Points of Particle Adhesion in Microvascular Networks

Balabhaskar Prabhakarpandian[1], **Yi Wang**[1], **Angela Rea-Ramsey**[1], **Shivshankar Sundaram**[1], **Mohammad F. Kiani**[2,3], and **Kapil Pant**[1]

[1] Biomedical Technology, CFD Research Corporation, 215 Wynn Dr. Huntsville AL 35805

[2] Department of Mechanical Engineering, Temple University, Philadelphia PA 19122

[3] Department of Radiation Oncology, Temple University, Philadelphia PA 19122

Abstract

Objective—Particle adhesion in vivo is dependent on microcirculation environment which features unique anatomical (bifurcations, tortuosity, cross-sectional changes) and physiological (complex hemodynamics) characteristics. The mechanisms behind these complex phenomena are not well understood. In this study, we used a recently developed in vitro model of microvascular networks, called Synthetic Microvascular Network, for characterizing particle adhesion patterns in the microcirculation.

Methods—Synthetic microvascular networks were fabricated using soft lithography processes followed by particle adhesion studies using avidin and biotin-conjugated microspheres. Particle adhesion patterns were subsequently analyzed using CFD based modeling.

Results—Experimental and modeling studies highlighted the complex and heterogeneous fluid flow patterns encountered by particles in microvascular networks resulting in significantly higher propensity of adhesion (>1.5X) near bifurcations compared to the branches of the microvascular networks.

Conclusion—Bifurcations are the focal points of particle adhesion in microvascular networks. Changing flow patterns and morphology near bifurcations are the primary factors controlling the preferential adhesion of functionalized particles in microvascular networks. Synthetic microvascular networks provide an in vitro framework for understanding particle adhesion.

Keywords

particles; adhesion; synthetic microvascular networks; bifurcation; flow; shear

INTRODUCTION

Particle (e.g. cell, drug carrier) adhesion to tissue (e.g. vascular endothelium) depends critically upon the geometric features of the vasculature at the site of adhesion and the associated local hemodynamic factors such as wall shear rate, dynamic pressure, and residence time. Understanding the complex interplay between these factors is critical to delivery of particulate carriers to the target site. However, the mechanisms responsible for the non-uniform distribution of adhering particles in microvascular networks are not clear in part because of a lack of appropriate in vitro models of microcirculation.

Corresponding author: Balabhaskar Prabhakarpandian, Biomedical Technology, CFD Research Corporation, 215 Wynn Dr, Huntsville, AL35805, bxp@cfdrc.com, Ph: 256-327-0665, Fax: 256-327-0985.

Traditionally, idealized *in vitro* flow chambers have been used to study particle adhesion [2, 16, 2]. These flow chambers have the benefit of readily characterized constant wall shear rate which can be used directly in the interpretation of experimental results, especially the generation of a shear adhesion map for the particles. Although these flow chambers have been used for over a decade for studying cellular and particle behavior [3,4, 7, 19, 25, 30, 31, 33], they have important short comings, most notably lack of correspondence with *in vivo* geometry (bifurcations, etc.), unrealistic scale/aspect ratios (microvasculature vs. large vessels), need for large reagent volumes, and inability to differentiate between adhesion patterns in healthy vs. diseased vasculature [6].

In recent years, several microfluidic devices mimicking microvessels have been developed [5,15 24, 27]. However, most of these devices feature linear channels or at best comprise of repetitive patterns of fixed angle bifurcations which do not accurately represent the complex topology observed in the microvasculature. Furthermore, although the findings from these devices provide important information on shear-dependent adhesion, detailed shear adhesion patterns cannot be obtained owing to the simplified constructs.

To overcome these limitations, we have recently developed a methodology for studying particle adhesion in a realistic in vitro model of the microvascular environment [20]. Vascular fluidic networks, obtained from digitization of *in vivo* microvascular topology, were prototyped using soft-lithography techniques [1] to obtain *in vitro* representation of microvascular networks (termed Synthetic Microvascular Networks or SMNs). Computational Fluid Dynamics (CFD) analyses of fluid flow and particle transport in the SMNs were used to provide detailed information on wall shear rates and particle fluxes in the entire network. The advantages of the SMNs over parallel plate flow chambers were also experimentally demonstrated for particle adhesion studies.

Microvascular networks commonly have a number of different diverging (a parent branch splitting into two daughter branches) and converging (two branches joining) bifurcations, which are the primary sites for binding of cells (platelets, leukocytes, etc.) under pathological conditions [28]. However, to our knowledge, the mechanisms for this preferential adhesion of particles near bifurcations have not been studied before. In a recent study [29], we showed that the adhesion patterns of leukocytes in vivo and particles in vitro using SMN at bifurcations are not due to the presence of endothelial cells and/or presence of various adhesion molecules. In this study, we used our novel SMN in conjunction with CFD modeling to investigate the effects of fluid dynamics and vascular geometry on particle adhesion patterns in microcirculation. One of the major aims of the current study was to investigate whether the non-uniformities in wall shear rates were responsible for this preferential adhesion of particles at the bifurcations. Particle adhesion profiles at the bifurcations were characterized and compared to particle adhesion in the branches of SMNs. Computational Fluid Dynamics (CFD) based simulations were used to estimate wall shear forces and their relationship to the observed adhesion patterns between bifurcation and branches.

MATERIALS AND METHODS

Digitization and Fabrication of SMN

Microvascular networks were digitized using the methods developed before [20]. Briefly, a microvascular network was randomly selected from a database of images of cremaster muscle of hamsters (Syrian Golden) collected according to the ANET system developed previously [18, 22, 23]. The images were traced and digitized using the software package Arc-Info (ESRI) into AutoCAD-MAP format. Flow directions in these networks as observed *in vivo* served as guidelines for defining inlet and outlet ports in the digitized network. The

networks used in these studies comprised of 100 μm width and depth in the channels. Layouts of the digitized network images were printed at high resolution on Mylar mask, which was then used to pattern a positive resist (AZ P4620, Clariant, Somerville, NJ) spun on top of a silicon wafer to create the masters for fabrication. The networks used in these studies comprised of channels of rectangular cross-section with 100 μm width and 100 μm depth. The channel depth was verified measured using a Dektakprofilometer (Veeco, Woodbury, NY) and was found to be within 3%.

Sylgard 184 PDMS was prepared according to manufacturer's instructions (Dow Corning, Midland, MI) and poured over the developed masters. The polymer was then degassed and allowed to cure overnight in an oven at 65°C to create complementary microchannels in PDMS. Through holes, defining the inlets and outlets, were cored using a 1.5mm punch (Ted Pella Inc., Redding, CA). Following plasma treatment (PDC-001, Ithaca, NY) for 30 seconds, the PDMS networks were bonded to a pre-cleaned 1×3 inches glass slide. Tygonmicrobore tubing (0.06 inch OD and 0.02 inch ID) connected to 30 gauge stainless steel needle served as the connecting port to the syringe mounted on a syringe pump (PHD 2000, Harvard Apparatus, MA).

Coating of SMN with Avidin

The inlet of the SMN chip was connected via tygonmicrobore tubing to a 1 mL syringe mounted on a syringe pump. An 8-port perfusion manifold (MPP-8, Harvard Apparatus MA) was connected to the outlets of the microvascular chip using microbore tubing. The inlet of the perfusion manifold was connected to a 1 mL syringe via the microbore tubing. A lab stand was used to clamp the 1 mL syringe in the vertical position above the chip with a removable clamp (Qosina, Edgewood, NY) on the tubing. Avidin (Invitrogen, Carlsbad, CA) at a concentration of 20 μg/ml was withdrawn into the vertical mounted syringe. To remove air from the manifold, each line was allowed to form a droplet before inserting into the network. This was repeated with all of the outlet tubings until there was no air left in the lines. The syringe pump was then set to refill at 1 μl/min for 10 minutes to allow perfusion of the SMN. At the end of the flow time, the device was wrapped in para film and stored at 4°C in a humidified dish overnight.

SMN Adhesion Assay

The coated SMN device was allowed to come to room temperature (~10 minutes). The device was submerged in a 100mm petri dish filled with PBS to remove the tubing to ensure no air bubbles entered the device. New tubing was then connected to the 8-port perfusion manifold and primed with PBS (via a syringe) until all the tubes were filled with PBS. The tubing from the manifold was inserted into the outlets of the network. The syringe filled with PBS was removed from the manifold and the tubing was then inserted into a small dish of PBS to maintain constant pressure. The entire setup was placed on a motorized stage (LEP Ltd, Hawthorne, NY) mounted on an inverted epi-fluorescence microscope (TE 2000, Nikon Instruments Inc., Melville, NY).

A solution of 2 μm biotinylated particles at a concentration of 5×10^5/mL was prepared in PBS and loaded into a 1 ml syringe. A second 1 mL syringe primed with PBS was connected to a 3-way valve (Upchurch Scientific, Oak Harbor, WA). One port served as a waste port and the second port of the valve was connected to one of the split arm of 1/16 inch Y-connector (Cole Parmer, Vernon Hills, IL). The second split arm of the connector was connected to a 1 ml syringe loaded with biotinylated particles. The single arm of the Y-connector was joined to a small piece of 1/16 inch PEEK tubing via compliant platinum-cured silicone Masterflex® tubing, Cole Parmer, Vernon Hills, IL). The connected syringes were then placed on a programmable syringe pump (PHD 200, Harvard Apparatus, MA) and

flow was set at 10 μl/min. The Y-connector was initially primed with PBS followed by the biotinylated particles by switching the 3-way valve connected to PBS to go to the waste port. The flow was gradually reduced to a rate of 2.5 μl/min (corresponding wall shear rates at this flow rate were calculated using the CFD model) and the PEEK tubing was inserted into the inlet of the network. The network inlet port was then monitored under the microscope. At the first sign of entry of particles into the network, a timer was started and the particles flow was continued for 3 minutes. At the end of 3 minutes, PBS from the 3-way valve was turned on to flow via the Y-connector into the inlet port and the flow from the particle syringe was stopped. PBS flush of particles was continued for about 3 minutes to wash off particles. At the end of the PBS wash, a scan of the entire SMN was performed using the automated stage at 4X objective. A cooled CCD camera, RetigaExi (Qimaging, Surrey, BC, Canada) was used for acquiring images. The entire process was automated using the NIKON Elements software (NIKON, Melville, NY)

Measurement of Particle Adhesion in SMN

The acquired images were post-processed using NIKON Elements software. A circular AOI of 200 μm diameter was created at each of the bifurcation in the SMN. This AOI of 200 μm is twice the diameter of the vessel, a common methodology based on the principal that it takes 2X diameter from a bifurcation for parabolic profile to be reestablished in a vessel [9]. The automated object count tool of the NIKON Elements software was used to count the number of particles in each of the bifurcation AOI. The particle counts were transferred to MS Excel for data analysis. Similarly, a particle count of the entire SMN using the automated object count was also performed.

CFD Modeling

A general-purpose Computational Fluid Dynamics (CFD) code, CFD-ACE+ [12], based on the Finite Volume Method (FVM) was used to discretize and solve the governing equations. A computational mesh for the microvascular network was created by importing network layouts in DXF format into CFD-GEOM, the grid generation module of CFD-ACE+. Computational models of the network with rectangular cross-section similar to the experimental channels were utilized. A three-dimensional hybrid mesh comprising of hexahedral and prismatic elements was created for subsequent simulation and analysis. Modules of fluid flow and particle transport (point particle and finite inertia model) and a customized, shear-rate-based, stochastic adhesion model were used. This adhesion model [20] captures the inherently probabilistic nature of particle/cell adhesion process. Briefly, in this model, the probability of particle adhesion is given by $P = \exp(-G/G_c)$ where P is the probability of particle adhesion; G is the local shear rate at the wall and G_c is the critical shear rate at the wall. Critical shear rate was defined as the rate required to remove adhered particles from an adhesive surface. Model parameters were used similar to our previous study [20]. During analysis, mesh refinement studies were performed to establish grid independence and the final results were obtained with a computational domain consisting of approximately 110,000 nodes. The wall mesh size was 5–10X times compared to the diameter of the particle used in the studies.

Statistical Analysis

Unless otherwise noted, data are presented as mean ± Standard Deviation (SD). Analysis of variance was used to determine significant differences between the experimental, simulated and theoretical results. All values of $P < 0.05$ were considered statistically significant.

RESULTS

Adhesion of Functionalized Particles to Synthetic Microvascular Networks

Figure 1 shows the first synthetic microvascular network (SMN1) used in the study which has one inlet and 7 outlets. At the inlet flow rate of 2.5 μl/min (t=0 min) it took approximately 30 seconds for the particles to be distributed uniformly in all the branches of the network. After 3 minutes of particle injection (t = 3 min) followed by 3 minutes of PBS injection (t = 6 min) into the inlet of the SMN, no particles were observed in the inlet branch indicating that the inlet branch was flushed of any particles. Hence, 6 minutes after the start of each experiment was taken as the time-point for imaging particle adhesion. Figure 2a shows the particle adhesion patterns at 6 minutes in the network and Figure 2b shows the post-processed images with the area of interest (AOI) of 200 μm at the individual bifurcations.

Estimation of Shear Values Using CFD

Figure 3 shows the computation domain used in the CFD simulation of particle adhesion in the same network (SMN1). Figure 4a shows a sample image of the flow rate distribution and Figure 4b shows the calculated wall shear rate values in the network. As a result of the progressive and complex flow splits and joining, the shear rate in the network is highly heterogeneous (range 0–400 s^{-1}), and markedly decreases downstream. Figure 4c illustrates the corresponding map of particle adhesion based on simulation, which was found to be minimal in high shear regions (e.g. near the inlet channels where shear rate >300 s^{-1}), and maximal in low shear regions indicating that fluidic shear strongly influences particle adhesion in these microvascular networks. We then plotted the average wall shear rate for the branches and the bifurcations (Figure 4d) which showed that the average wall shear rate in branches was not significantly different from that in bifurcations.

Comparing Experimental and Simulated Particle Adhesion Patterns

A common approach for understanding preferential particle deposition at respiratory airway bifurcations is the deposition enhancement factor [32]. This approach states that if the particle adhesion patterns near bifurcations are similar to other parts of the network, then the deposition enhancement factor should be unity. To elucidate the impact of bifurcations on particle adhesion patterns in a microvascular network environment, a bifurcation adhesion ratio (BAR), similar to the deposition enhancement factor was defined, using the following equation:

$$BAR = \frac{Number\ of\ Particles\ Adhered\ in\ Bifurcations}{Number\ of\ Particles\ Adhered\ in\ the\ Entire\ SMN}$$

If particles do not exhibit any preferential adhesion near the bifurcations, the expected BAR should be approximately equal to the ratio of the area of the bifurcation to the area of the entire microvascular network. BAR values were calculated from both CFD simulations and experiments. The computational domain used for the CFD simulation was used to calculate total surface area of the 200 μm bifurcation AOIs as well as the entire network. The surface area occupied by bifurcations was calculated to be 1.6×10^{-6} m^2 and the surface area of the entire microvascular network was calculated to be $7.7\times10^{-6} m^2$. Figure 5a shows that the number of particles per unit area at the bifurcations is significantly higher than the number of particles per unit area of the branches.

However, as seen from Figure 5b, both experimental (BAR value of 49%) and simulation results (BAR value of 67%)showed significantly higher particle adhesion in bifurcations

compared to the expected value (BAR value of 24%). In order to test if this result was reproducible, we used a second microvascular network (SMN2, shown in Figure 6) to test the preferential adhesion patterns of particles at bifurcations. Again, as shown in Figure 7, both experimental (BAR value of 36%) and simulation (BAR value of 52%) findings indicate a significantly higher particle adhesion index compared to the expected value (21%).

To elucidate this particle adhesion patterns, we looked at detailed fluid velocity vectors in the microvascular network. Figure 8 shows complex velocity vectors in different regions of SMN1 exhibiting flow disturbances and complex flow patterns near the bifurcations for both low and high shear regions of the SMN. These complex and heterogeneous flow patterns present primarily due to the developing flow following flow split at the bifurcations in these networks can be attributed to the higher adhesion at the bifurcations. Similar observations have been reported in studies using lung airway models for both turbulent and laminar flows [13,32], where adhesion of micro particles at bifurcations is significant higher due to the impaction with the walls of vessels. Our results showing higher adhesion at the bifurcations suggest that these flow disturbances at the bifurcations cause the micro particles to impact the walls leading to higher adhesion compared to branches of the network.

Since networks are comprised of multiple bifurcations, we investigated further if a construct comprised of only a single bifurcation would provide similar preferential particle adhesion patterns. Hence, a bifurcating microfluidic device with 100 μm width and 50 μm depth in the parent branch and daughter channels with 50 μm width and 50 μm depth with a bifurcation angle of 30° was fabricated for testing (Figure 9). This simplified construct, termed Idealized Microvascular Network (IMN), can be considered as basic unit of a microvascular network.

Adhesion of biotinylated particles to the IMN was characterized as before except that the shear rates in the parent branch were varied from 240 sec^{-1} to 15 sec^{-1}. Each shear rate was held constant for 3 minutes and adhesion patterns (particles bound per unit area) at two AOIs were measured: (a) A circular AOI of 200 μm which is twice the width of the channel and sufficiently larger than the area of fluid disturbance expected from CFD simulations (data not shown), and (b) a rectangular AOI of 200 μm (length) × 100 μm (width of channel) in the middle of the strait section of the inlet channel. As shown in Figure 10, and consistent with results obtained in SMNs, functionalize particles preferentially adhere near bifurcations in comparison with the branches even in this simple bifurcation.

DISCUSSION

We recently developed a methodology for studying particle and cell adhesion in vitro in synthetic microvascular networks using a combination of microfluidics and CFD based simulations [20, 21]. In this study, we characterized spatial adhesion patterns of functionalized model drug carriers to test the hypothesis that that shear forces are the primary controllers of preferential particle adhesion in bifurcating regions in microvascular networks. Both experimental results with SMNs and CFD simulation studies highlight the fact that particles tend to preferentially adhere in bifurcations compared to branches of the microvascular networks. Particle adhesion patterns in the microvascular networks are highly non-uniform and significantly higher (>1.5) concentration of adhered particles was observed at bifurcations compared to the branches of the network. The complex and heterogeneous flow patterns in SMN observed using CFD modeling showed higher particle adhesion in low shear regions and minimal adhesion in high shear regions. These results are in agreement with linear flow chambers indicating an inverse relationship between levels of shear and particle adhesion [10]. However, our findings that even when wall shear rates are similar in

bifurcations and branches particles still adhere predominantly in bifurcations suggest that particle adhesion experiments performed using linear flow chambers might significantly underestimate particle adhesion in vivo and not be representative of adhesion patterns in microvascular networks. The results obtained with the simple bifurcating IMN also validate the hypothesis that particle adhesion patterns in microvascular networks are localized near bifurcations.

These findings also support the hypothesis that the geometrical features and changing flow conditions in bifurcations are responsible for the preferential adhesion of functionalized particles near bifurcations. Previously, we have shown that the presence or absence of endothelial cells and/or receptor concentrations on their surfaces, are not the driving forces behind the preferential adhesion patterns of leukocytes near bifurcations [29]. Other studies have shown that particle adhesion decreases with the particle size according to the relationship $d^{-1.7}$ where "d" is the diameter of the particle [4]. In addition, studies using lung airway models have shown that microparticles adhere at bifurcations with significantly higher propensity for both turbulent and laminar flow regimes [32] due to flow disturbances at the bifurcations. Hence, the higher adhesion of particles at the bifurcation observed in SMN is also likely the result of these altered flow patterns, which in turn lead to higher impaction at the walls of the bifurcations in the SMN.

Even though a simplified bifurcating channel can provide some information on preferential adhesion of particles in bifurcations, studying adhesion in complete microvascular networks such as SMN provides a more complete understanding of the dynamics of particle adhesion in the microcirculation. For example, differences in adhesion ratios in different size vessels and different angles of bifurcation can only be characterized *in vitro* in a fluidic device such as the one used in our study. Further studies are required to understand the effects of vessel tortuosity and cross-sectional changes on particle adhesion in different parts of the network. In addition, since most of the drug delivery vehicles are in the nanometer range, a size dependent study should be performed to determine if the preferential adhesion of functionalized particles near bifurcations is size dependent. This will be of particular relevance for nano particles, where different phenomenon such as Brownian diffusion, not seen with microparticles, may influence particle transport and adhesion patterns. SMNs can also be used to study the complex nature of cell adhesion assays, such as leukocyte-endothelial interactions, tumor-endothelial interactions and nano particle adhesion to cells in vitro which can be then validated in vivo.

CONCLUSIONS

The current study, in agreement with our previous in vivo studies, indicates that bifurcations are the focal points of cell and particle adhesion in microvascular networks. Results from experimental and simulation studies presented here indicate that changing flow patterns near bifurcations are the primary factors controlling the preferential adhesion of functionalized particles and leukocytes to bifurcation regions in microvascular networks. Synthetic microvascular networks, coupled with CFD simulations, can be used as an effective in vitro tool to characterize cell/particle adhesion in conditions mimicking the in vivo microcirculatory environment.

Acknowledgments

We thank Dr. Daniel Irimia of BioMEMS Resource Center, Massachusetts General Hospital for help with the fabrication of masters of the device. We acknowledge financial support from NIH (2R44HL076034-03) and the American Heart Association.

References

1. Anderson JR, Chiu DT, Jackman RJ, Cherniavskaya O, McDonald JC, Wu H, Whitesides SH, Whitesides GM. Fabrication of topologically complex three-dimensional microfluidic systems in PDMS by rapid prototyping. Anal Chem. 2000; 72(14):3158–64. [PubMed: 10939381]
2. Chau L, Doran M, Cooper-White J. A novel multi shear microdevice for studying cell mechanics. Lab Chip. 2009; 9(13):1897–902. [PubMed: 19532965]
3. Cuvelier SL, Patel KD. Studying leukocyte rolling and adhesion in vitro under flow conditions. Methods Mol Biol. 2005; 290:331–42. [PubMed: 15361672]
4. Decuzzi P, Gentile F, Granaldi A, Curcio A, Causa F, Indolfi C, Netti P, Ferrari M. Flow chamber analysis of size effects in the adhesion of spherical particles. Int J Nanomedicine. 2007; 2(4):689–96. [PubMed: 18203435]
5. Emerson DR, Cieślicki K, Gu X, Barber RW. Biomimetic design of microfluidic manifolds based on a generalised Murray's law. Lab Chip. 2006; 6(3):447–54. [PubMed: 16511629]
6. Fukumura D, Jain RK. Imaging angiogenesis and the microenvironment. APMIS. 2008; 116(7–8): 695–715. [PubMed: 18834413]
7. Gentile F, Curcio A, Indolfi C, Ferrari M, Decuzzi P. The margination propensity of spherical particles for vascular targeting in the microcirculation. J Nanobiotechnology. 2008; 15(6):9. [PubMed: 18702833]
8. Goetz DJ, Greif DM, Shen J, Luscinskas FW. Cell-cell adhesive interactions in an in vitro flow chamber. Methods Mol Biol. 1999; 96:137–45. [PubMed: 10098131]
9. Lew HS, Fung YC. Entry flow into blood vessels at arbitary Reynolds number. J Biomech. 1970; 3:22–38.
10. Ham AS, Goetz DJ, Klibanov AL, Lawrence MB. Microparticle adhesive dynamics and rolling mediated by select in-specific antibodies under flow. 2007; 96(3):596–607.
11. Hyduk SJ, Cybulsky MI. Role of alpha4beta1 integrins in chemokine-induced monocyte arrest under conditions of shear stress. Microcirculation. 2009; 16(1):17–30. [PubMed: 18979279]
12. Jiang, Y.; Przekwas, AJ. Implicit, pressure-based incompressible Navier-Stokes solver for unstructured meshes, AIAA-94–0303. 1994.
13. Kleinstreuer C, Zhang Z. An adjustable triple-bifurcation unit model for air-particle flow simulations in human tracheobronchial airways. J Biomech Eng. 2009 Feb.131(2):021007. [PubMed: 19102566]
14. Kreke MR, Sharp LA, Lee YW, Goldstein AS. Effect of intermittent shear stress on mechanotransductive signaling and osteoblastic differentiation of bone marrow stromal cells. Tissue Eng Part A. 2008; 4(4):529–37. [PubMed: 18352827]
15. Lim D, Kamotani Y, Cho B, Mazumder J, Takayama S. Fabrication of microfluidic mixers and artificial vasculatures using a high-brightness diode-pumped Nd:YAG laser direct write method. Lab Chip. 2003; 3(4):318–23. [PubMed: 15007466]
16. Liu D, Wang L, Zhong R, Li B, Ye N, Liu X, Lin B. Parallel microfluidic networks for studying cellular response to chemical modulation. J Biotechnol. 2007; 131(3):286–92. [PubMed: 17706314]
17. Man S, Tucky B, Bagheri N, Li X, Kochar R, Ransohoff RM. alpha4 Integrin/FN-CS1 mediated leukocyte adhesion to brain microvascular endothelial cells under flow conditions. J Neuroimmunol. 2009; 210(1–2):92–9. [PubMed: 19345424]
18. Nguyen V, Gaber MW, Sontag MR, Kiani MF. Late effects of ionizing radiation on the microvascular networks in normal tissue. Radiat Res. 2000; 154(5):531–6. [PubMed: 11025649]
19. Prabhakarpandian B, Goetz DJ, Swerlick RA, Chen X, Kiani MF. Expression and functional significance of adhesion molecules on cultured endothelial cells in response to ionizing radiation. Microcirculation. 2001; 8(5):355–64. [PubMed: 11687947]
20. Prabhakarpandian B, Pant K, Scott RC, Patillo CB, Irimia D, Kiani MF, Sundaram S. Synthetic microvascular networks for quantitative analysis of particle adhesion. Biomed Microdevices. 2008; 10(4):585–95. [PubMed: 18327641]

21. Rosano JM, Tousi N, Scott RC, Krynska B, Rizzo V, Prabhakarpandian B, Pant K, Sundaram S, Kiani MF. A physiologically realistic in vitro model of microvascular networks. Biomed Microdevices. 2009; 11(5):1051–1057.
22. Roth NM, Kiani MF. A “geographic information systems” based technique for the study of microvascular networks. Ann Biomed Eng. 27(1):42–7. [PubMed: 9916759]
23. Roth NM, Sontag MR, Kiani MF. Early effects of ionizing radiation on the microvascular networks in normal tissue. Radiat Res. 1999; 151(3):270–7. [PubMed: 10073664]
24. Runyon MK, Johnson-Kerner BL, Ismagilov RF. Minimal functional model of hemostasis in a biomimetic microfluidic system. Angew Chem Int Ed Engl. 2004; 43(12):1531–6. [PubMed: 15022225]
25. Sakhalkar HS, Dalal MK, Salem AK, Ansari R, Fu J, Kiani MF, Kurjiaka DT, Hanes J, Shakesheff KM, Goetz DJ. Leukocyte-inspired biodegradable particles that selectively and avidly adhere to inflamed endothelium in vitro and in vivo. Proc Natl Acad Sci U S A. 2003; 100(26):15895–900. [PubMed: 14668435]
26. Sarvepalli DP, Schmidtke DW, Nollert MU. Design considerations for a microfluidic device to quantify the platelet adhesion to collagen at physiological shear rates. Ann Biomed Eng. 2009; 37(7):1331–41. [PubMed: 19440840]
27. Schaff UY, Xing MM, Lin KK, Pan N, Jeon NL, Simon SI. Vascular mimetics based on microfluidics for imaging the leukocyte--endothelial inflammatory response. Lab Chip. 2007; 7(4): 448–56. [PubMed: 17389960]
28. Sharma SK, Sweeny J, Kini AS. Coronary bifurcation lesions: a current update. Cardiol Clin. 2010; 28(1):55–70. [PubMed: 19962049]
29. Tousi N, Wang B, Pant K, Kiani MF, Prabhakarpandian B. Preferential adhesion of leukocytes near bifurcations is endothelium independent. Microvasc Res. 2010 Dec; 80(3):384–8. [PubMed: 20624406]
30. Wiese G, Barthel SR, Dimitroff CJ. Analysis of physiologic E-selectin-mediated leukocyte rolling on microvascular endothelium. J Vis Exp. 2009; 11(24):pii, 1009. [PubMed: 19229187]
31. Zeng W, Li L, Yuan W, Wei Y, Mi J, Sun J, Wen C, Zhang W, Ying D, Zhu C. A20 over expression inhibits low shear flow-induced CD14-positive monocyte recruitment to endothelial cells. Biorheology. 2009; 46(1):21–30. [PubMed: 19252225]
32. Zhang Z, Kleinstreuer C, Donohue JF, Kim CS. Comparison of micro- and nano-size particle depositions in a human upper airway model. J Aerosol Sci. 2005; 36:211–233.
33. Zou X, Shinde Patil VR, Dagia NM, Smith LA, Wargo MJ, Interliggi KA, Lloyd CM, Tees DF, Walcheck B, Lawrence MB, Goetz DJ. PSGL-1 derived from human neutrophils is a high-efficiency ligand for endothelium-expressed E-select in under flow. Am J Physiol Cell Physiol. 2005; 289(2):C415–24. [PubMed: 15814589]

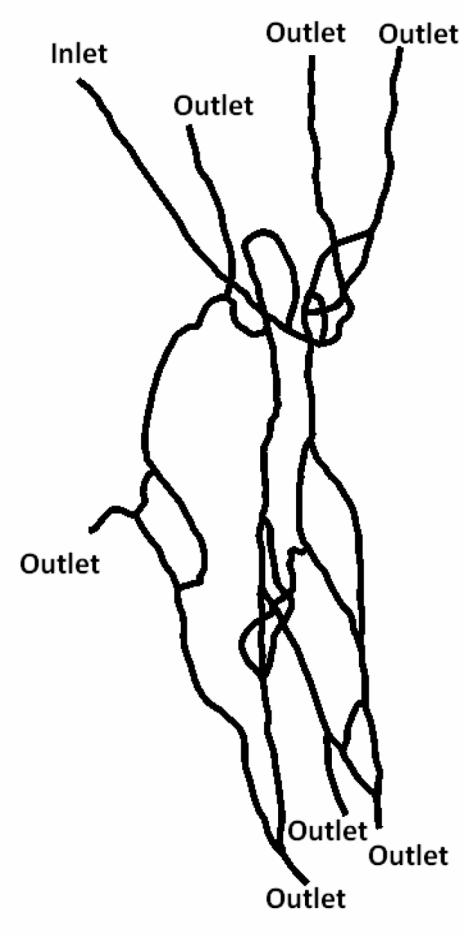

Figure 1.
First synthetic microvascular network (SMN1) used in the particle adhesion study

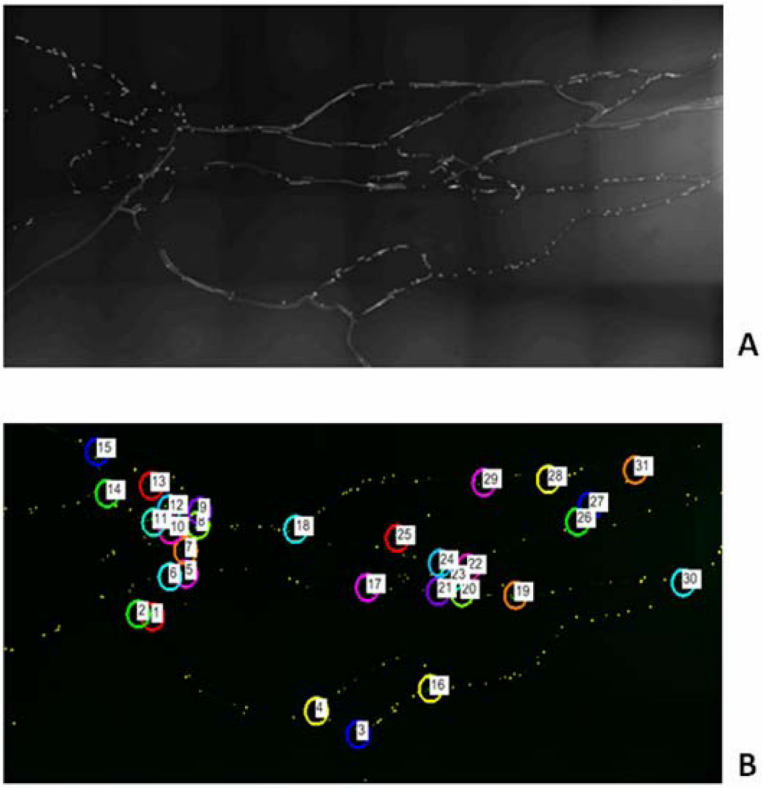

Figure 2.
A. Raw Image of SMN1 with adhered biotinylated particles 6 minutes post injection.
B. Post-processed images with highlighted AOIs in the bifurcations of SMN1.

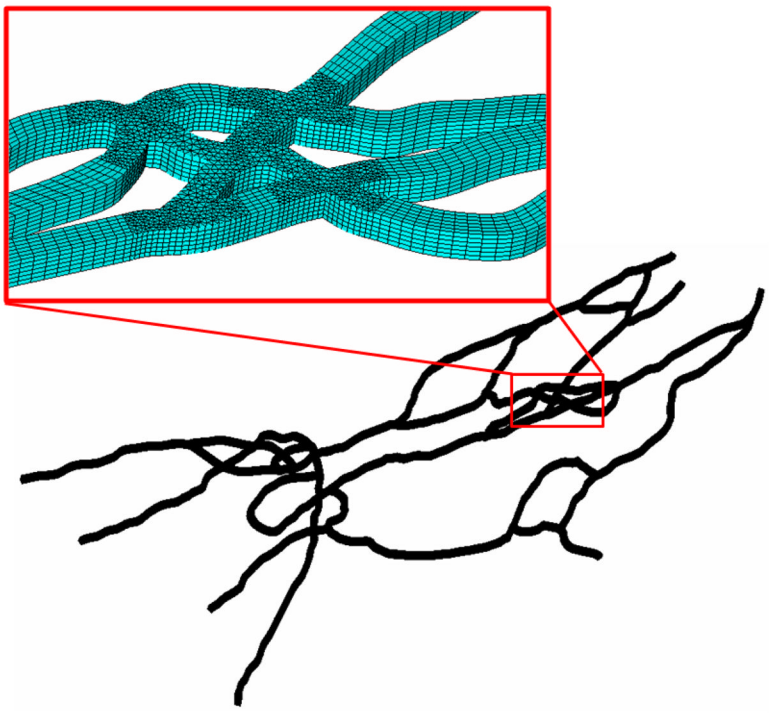

Figure 3.
A typical computational mesh of the microvascular networks (~110,000 computational cells) used in the CFD simulation.

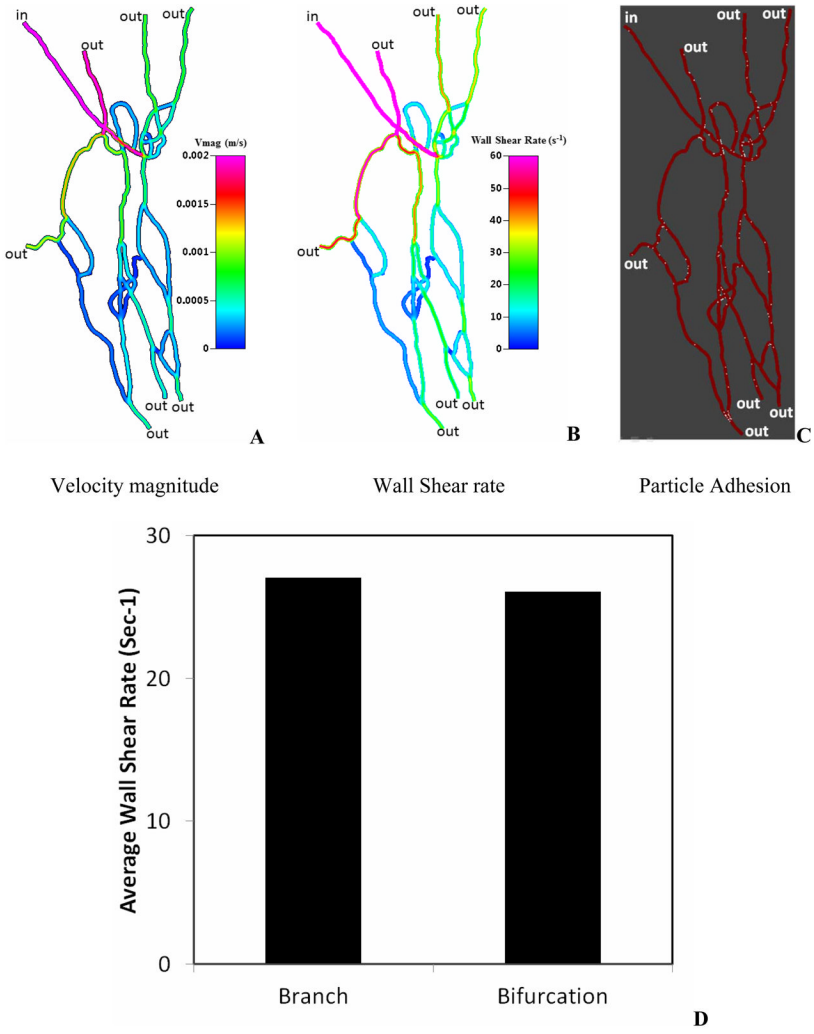

Figure 4.

CFD Simulation results in the SMN1.

A. Distribution of velocity magnitude (equivalent to the flow rate) ranging from 0 to 2mm/s

B. Distribution of wall shear rate at the top surface of the vessel ranging from 0 to 60 sec^{-1}

C. Sample results of particle adhesion patterns

D. Average wall shear rate comparison between branches and bifurcations indicating no significant differences

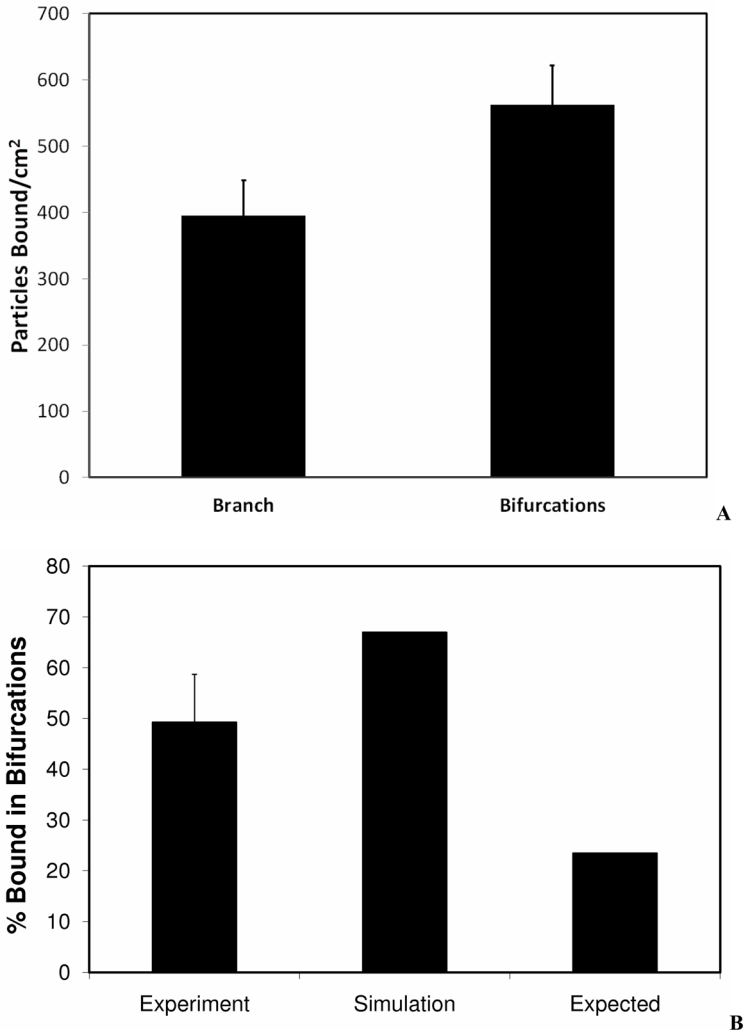

Figure 5.

Particle adhesion in SMN1.

A. Adhesion per unit surface area for branches vs. bifurcations. Particles adhered in significantly larger numbers at bifurcations compared to branches of SMN. Experimental results are averaged from three runs with error bars representing standard deviation.

B. Comparison of adhesion patterns. Expected values are based on theoretical calculations assuming no effect of bifurcations on the adhesion. Simulation values are based on CFD results. Experimental results are averaged from three runs with error bar representing standard deviation. Percentage of particles adhered in bifurcations for both experimental (49%) and simulation (67%) was significantly higher than the expected (24%) values.

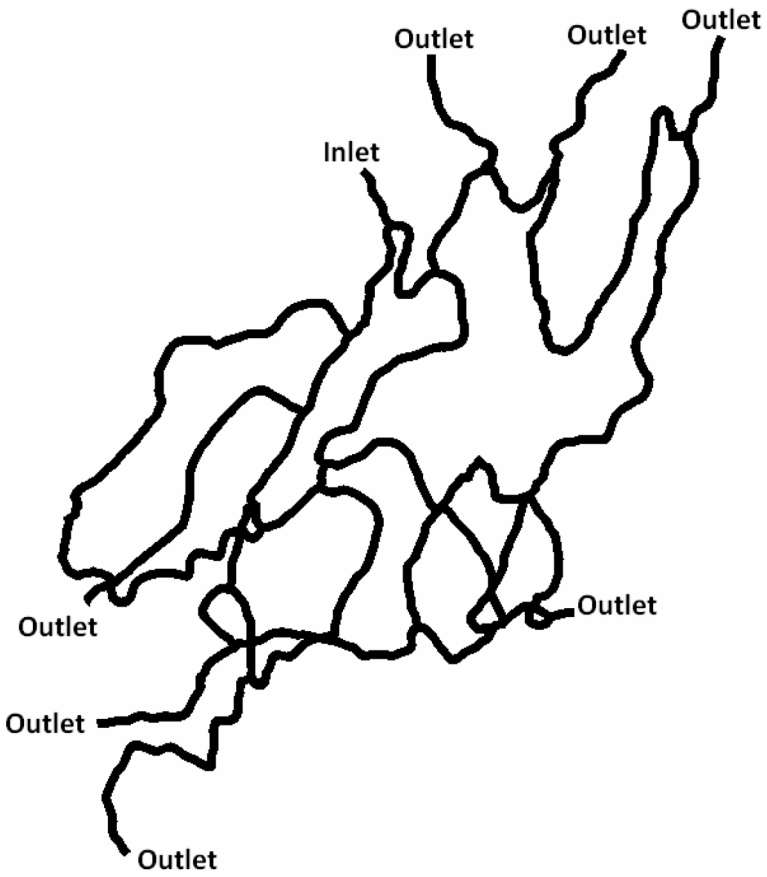

Figure 6.
Second synthetic microvascular network (SMN2) used in the particle adhesion study

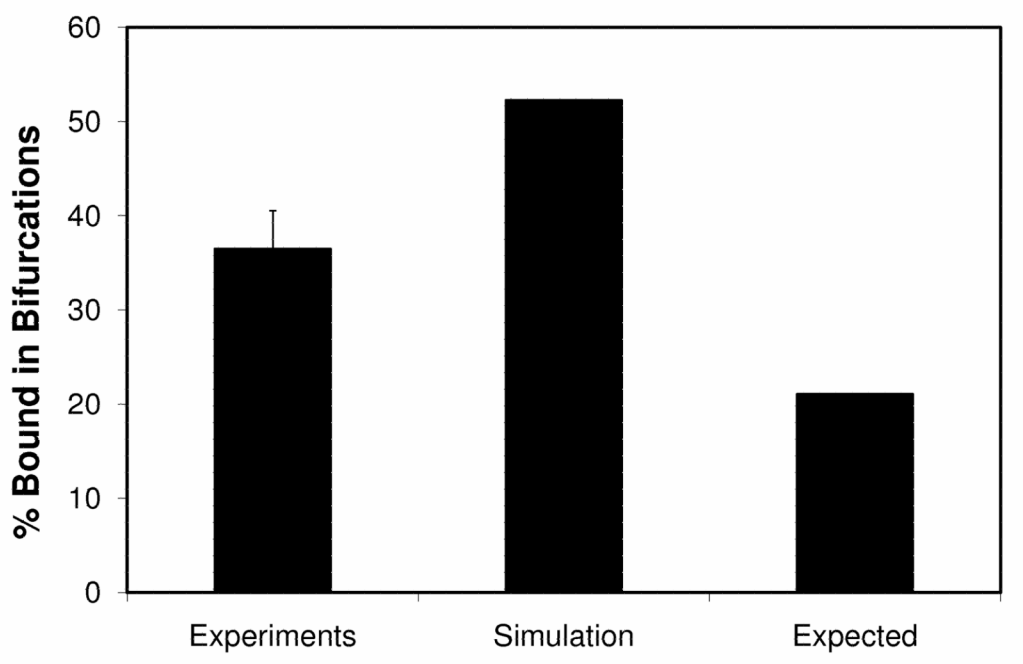

Figure 7.

Particle adhesions in SMN2. Expected values are based on theoretical calculations assuming no effect of bifurcations on the adhesion. Simulation values are based on CFD results. Experimental results are averaged from three runs with error bar representing standard deviation. Percentage of particles adhered in bifurcations for both experimental (36%) and simulation (52%) was significantly higher than the expected (21%) values.

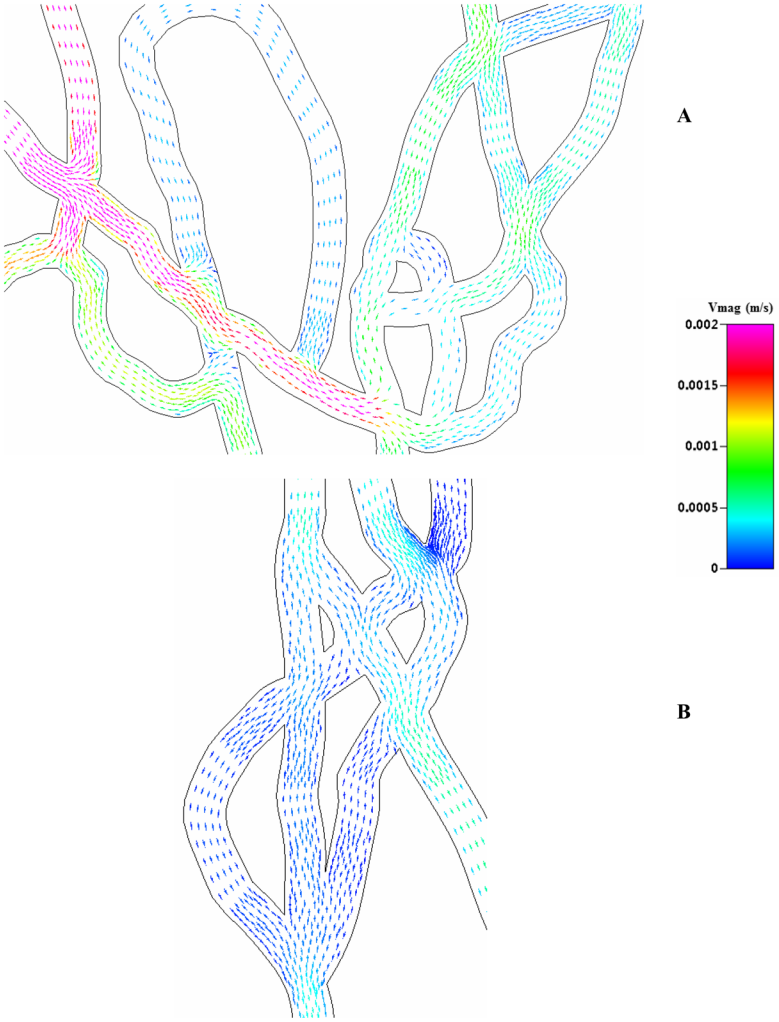

Figure 8.
Fluid velocity vectors in different sections of SMN1. The vectors are colored by velocity magnitude ranging from 0 to 2mm/s. Complex and heterogeneous fluidic patterns are present in the entire network near the bifurcations, for both the high (Figure A) and low flow rate (Figure B) regions.

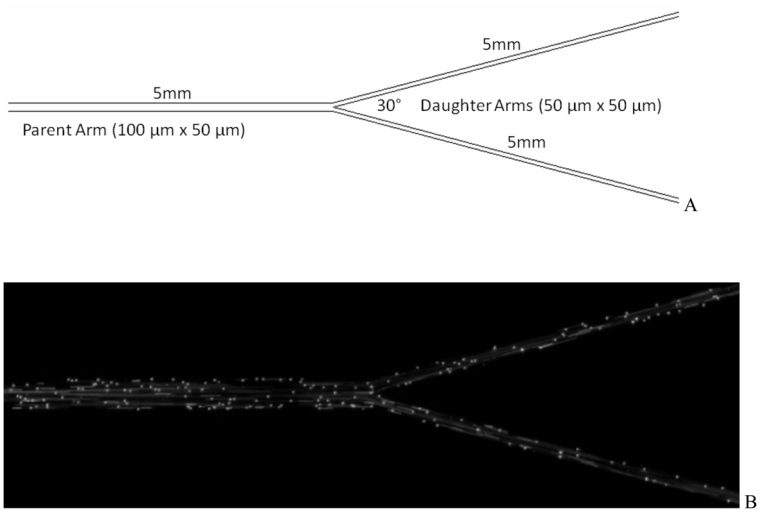

Figure 9.
Panel A, Schematic of the idealized microvascular network (IMN).
Panel B, Image of fluorescent particle adhesion in IMN. The flow is from left to right in the figure.

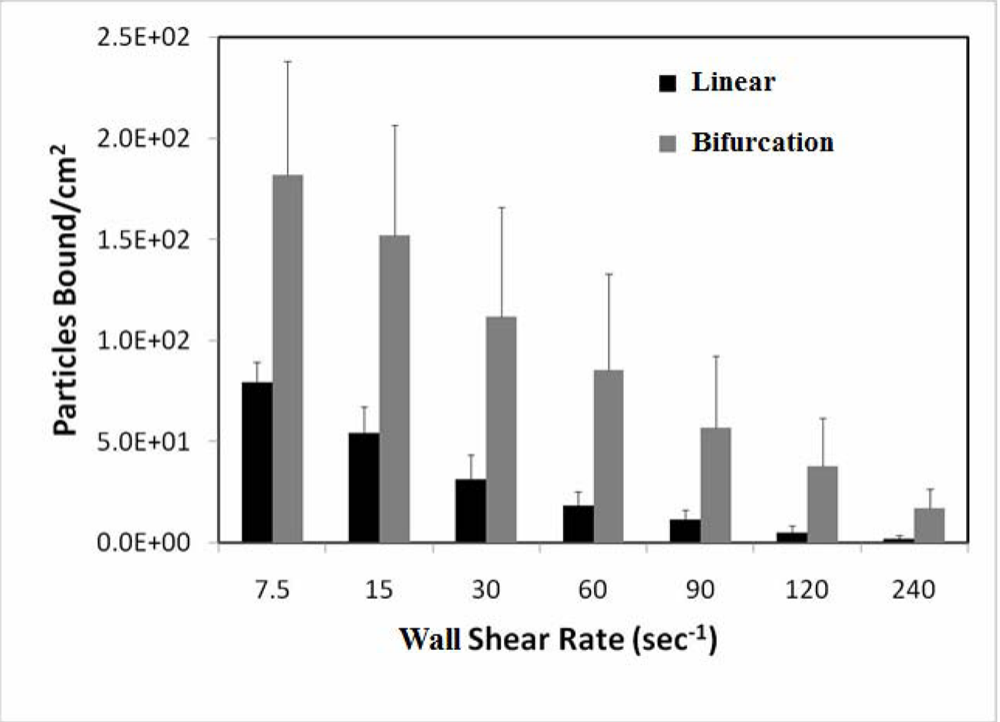

Figure 10.
Adhesion patterns in bifurcation and linear section of IMN. Particles adhere in significantly larger numbers in bifurcations than linear sections at all shear rates. Experimental results are averaged from three runs with error bars representing standard deviation.